Heliyon 10 (2024) e38541

Contents lists available at ScienceDirect

Heliyon

journal homepage: www.cell.com/heliyon

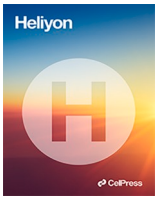

Research article

Unveiling the therapeutic potential of *Canavalia rosea* leaves: Exploring antioxidant, anti-inflammatory, anti-arthritic, and cytotoxic activities through biological and molecular docking evaluation with DFT analysis

Nasim Sazzad [a], Fowzul Islam Fahad [a], Shahenur Alam Sakib [a], Mohammed Abu Tayab [a], Md. Abu Hanif [a], A.S.M. Ali Reza [a,**], Mohammad Nazmul Islam [a,c,***], Raffaele Capasso [b,*]

[a] *Department of Pharmacy, International Islamic University Chittagong, Chittagong, 4318, Bangladesh*
[b] *Department of Agricultural Sciences, University of Naples Federico II, 80055, Portici, Naples, Italy*
[c] *Department of Pharmacy, Jahangirnagar University, Savar, Dhaka 1342, Bangladesh*

ARTICLE INFO

Keywords:
Canavalia rosea
Antioxidant
Anti-inflammatory
Anti-arthritic
Cytotoxicity
Molecular docking

ABSTRACT

Background: *Canavalia rosea* is a common tropical seacoast flowering plant from the family of Fabaceae which is reported as bay bean and coastal jack bean; has a wide range of therapeutic and nutraceutical properties.
Aim: The present research aims to explore some pharmacological insights of the methanol extract *C. rosea* of leaves (MECR) and its chloroform fraction (CFCR) and n-hexane fraction (NFCR) through *in-vitro* and *in-silico* approaches.
Methods: Different fractions of *C. rosea* were subjected to ferric reduction assay and total phenolic and flavonoid content assay to explore their antioxidant potential. The anti-inflammatory activity was assessed on the hypotonic-induced human erythrocyte-lysis model, while the protein denaturation method was applied for screening anti-arthritis properties of plant extract; and the cytotoxic activity was evaluated by brine shrimp lethality bioassay. In the in-silico study, molecular docking, pass prediction and ADME/T, analysis was used to investigate anti-arthritic, anti-inflammatory, antioxidant and cytotoxic potency of five selected compounds of *C. rosea*. Finally, the quantum chemical density functional test analysis was applied to investigate the chemical and physical properties of those compounds.
Results: All the soluble organic extracts of *C. rosea* demonstrated moderate toxicity with strong antioxidants potential, in which MECR manifested the peak level of scavenging activity (2.49) on ferric reduction assay. MECR, CFCR & NFCR significantly protected lysis of human erythrocyte membrane induced by hypotonic solution, whereas MECR and CFCR were exhibited partially equal inhibitory activity. The *in-vitro* anti-arthritis assay, MECR, NFCR and CFCR showed strongly significant ($p<0.001$) inhibitory potency at 500 μg/mL & 1000 μg/mL concentrations. The molecular docking simulations revealed strong binding of all compounds to specific receptors, with Rutin showing the highest biological reactivity followed by Daucosterol, β-Sitosterol,

* Corresponding author.
** Corresponding author.
*** Corresponding author. Department of Pharmacy, International Islamic University Chittagong, Chittagong, 4318, Bangladesh.
E-mail addresses: alirezaru@gmail.com (A.S.M.A. Reza), nazmul@iiuc.ac.bd (M.N. Islam), rafcapas@unina.it (R. Capasso).

https://doi.org/10.1016/j.heliyon.2024.e38541
Received 6 October 2023; Received in revised form 6 September 2024; Accepted 25 September 2024
Available online 26 September 2024

Stigmasterol, and Guanidine. All the compounds showed favorable reactivity patterns, with O and H atoms poised for nucleophilic and electrophilic attacks in chemical density functional calculations.

Conclusion: The recent investigation suggests that *C. rosea* could have the potential source of antioxidant, anti-inflammatory, anti-arthritis and cytotoxic activity, prompting further investigation into their mechanisms.

1. Introduction

The existence of free radicals in human body was just discovered within last 50 years [1]. Molecules such as reactive oxygen and nitrogen species (RONS) can be considered as free radicals which act as a crucial role in biological evolution and also exert some beneficial action against several organisms [2]. But the excess production of free radicals may damage biomolecules (e.g., DNA, lipids, protein, etc.) and develop oxidative stress in human body. As a result, the redox homeostasis in the tissue became imbalance which can generate a range of disorders like neurodegenerative diseases, diabetes, rheumatoid arthritis, cardiovascular diseases, atherosclerosis, chronic inflammation, and cancer [3]. Cell membrane proteins play a vital role in cell physiology. Cells produce their lysosomal enzymes that lead to tissue damage and thus results inflammation. It is recognized as cell membrane stabilization inhibits lysis and successive phospholipases release that restrict the scheme of tissue damage and inflammation [4,5]. However, another considerable issue is oxidative stress for producing inflammation in the body. Inflammation cells at a pathological condition generate nitric oxide radical (*NO) and oxygen radical (O_2^{-1}) which subsequently produce a potent oxidizing agent "peroxy-nitrite anion ($ONOO^{-1}$)". This anion further disseminates into nitrosonium cations (NO^{+1}) and nitroxyl anions (NO-1) through DNA fragmentation and lipid peroxidation, thereby inducing OS and physiological dysfunctions [6]. Besides, a group of oxidative enzymes recognizes as Lipoxygenases (LOXs) that generate pro-inflammatory mediators and regulate inflammatory responses. And, these enzymes are contribute to the onset of psoriasis, rheumatoid arthritis, and asthmatic responses by reducing the formation of hydro-peroxy-eicosatetraenoic acids (HPETEs) from arachidonic acid [7,8]. Unfortunately, plenty of synthetic classes of drugs like non-steroidal anti-inflammatory drugs (NSAIDs), corticosteroids and disease-modifying anti-rheumatic drugs (DMARDs), etc., utilized arthritis and inflammation treatment have potential side effects and limited effectiveness, so researchers are turning to natural sources for safer and more potent alternatives [9]. Interestingly, naturals products are used to develop new therapeutic entities over the century. Plenty of secondary metabolites are developed from medicinal plant origin which manifests better potency, safety in comparison with synthetic medicines [10]. Hence, the agents which have the potential of stabilization of cell membrane, anti-arthritis properties with RONS ameliorating activity could the most suitable option for the management of anti-arthritic and anti-inflammatory response.

Canavalia rosea is a very common tropical seacoast plant which reported as beach bean, bay bean, coastal jack bean and seaside jack-bean. It is a flowering plant from the family of Fabaceae; mainly grows in the coastal area which is situated in the tropics and subtropics throughout the world. Due to the potentiality of this plant, it can be widely used as fodder, fertilizer, food and medicinal purposes [11]. *C. rosea* has toxins for which aboriginals soak the plant in the water to catch fishes. It also contains antioxidants such flavonoids, tannins, lignins, vitamin A, vitamin C and vitamin E revealed in studies [12]. The leaves of *C. rosea* shows antimicrobial activity against various microorganisms like *S. aureus, S. faecalis, B. cereus, B. megaterium*. Canarosine, a chemical compound extracted from *C. rosea* caused maximum inhibition (95 %) of dopamine-1 receptor binding and the alkaloids from the plant were active against *P. falcifarum* K1 strain with a moderate activity against that of Herpes simplex virus type-1 [12]. Nevertheless, the plant has many beneficial traditional practices, as yet, no scientific investigation has been carried out to explore its effects against inflammation and arthritis disorders. Hence, this study was designed to evaluate the antioxidant, anti-inflammatory, anti-arthritis, and cytotoxic effects of various soluble organic fractions of *C. rosea* using in vitro experimental models, alongside in silico molecular docking and optimization to identify potential lead compounds.

2. Methods & materials

2.1. Chemicals & equipment

Methanol, hydrochloric acid, sodium carbonate, sodium phosphate, sodium chloride, sulfuric acid & potassium ferricyanide were purchased from Merck (Germany). Ascorbic acid, ferric chloride, sodium acetate and trichloro-acetic-acid (TCA) were collected from Sigma chemical co. (USA). Diclofenac sodium was gained from Square Pharmaceutical Ltd. (Bangladesh). Vincristine sulphate was purchased from Beacon Pharmaceutical Ltd. (Bangladesh). Plenty of chemicals subjected in this experiment are analytical grade with specified references. Ultra Violet-Vis-Spectrophotometer (UVmini-1240, Shimadzu, Japan) was employed to analyze the absorbance of this investigation.

2.2. Plant collection and extracts preparation

C. rosea leaves were obtained from the Mirsharai, Chittagong, Bangladesh in March 2019 which was authenticated by renowned taxonomist Prof. Dr. Shaikh Bakhtiar Uddin, University of Chittagong, Chittagong, Bangladesh. The fresh leaves of the plant were dried about 10 days under shade at low temperature, and then ground into fine powder. Then, the air-dried powdered were extracted with

water-methanol (3:7) mixture using a shaker for 2 weeks, and filtered through cotton and Withman filter paper respectively. After that, the filtrate was evaporated at 40-50 °C temperature. Thus, it yields a residue characterized as methanol extract of *C. rosea* (MECR), which was kept in a refrigerator for further study.

The solvent-solvent partitioning protocol was designed by the method of Kupchan et al. [13], and modified Van Wagenen et al. [14]. The n-hexane fraction (NFCR) and chloroform fraction (CFCR) were subjected to evaporate for further experimental analysis. The total yields value of MECR, NFCR and CFCR were 8.21, 1.15 and 0.85 g respectively. The P&D committee (Pharm-P&D17/08'-19), Department of Pharmacy, International Islamic University Chittagong, Chittagong, Bangladesh., has authorized and certified every methodology and design of this study.

2.3. Preliminary phytochemical screening

The methanol extract of *C. rosea* leaves (MECR) was experimented for qualitative phytochemical analysis through the standard determination methods of phytochemicals (e.g., carbohydrates, alkaloids, tannins, reducing sugar, phenols, flavonoids, saponins, glycosides, protein, etc.) [15].

2.4. In-vitro antioxidant activity

2.4.1. Ferric-reducing power capacity (FRPC)

The reducing power ability was analyzed by the Oyaizu technique [16]. 2.5 mL of 1 % potassium ferricyanide and phosphate buffer were added to 1 mL of the crude extract at different concentrations (62.5–1000 μg/mL), and the mixture solution was then incubated at 50 °C. After the mixture had been incubated, 2.5 mL of a 10 % trichloroacetic acid (TCA) solution was added again, and then the mixture was centrifuged for 10 min at 3000 rpm. The upper layer (supernatant solution) of the mixture was withdrawn after centrifuging, and added 2.5 mL of distilled water with half milliliters of freshly prepared ferric chloride (1 %). The absorbance was allowed to measure at 700 nm where ascorbic acid was applied as the standard drug.

2.4.2. Total phenolic content test

The total phenolic content of plant extract was measured by the following method, where galic acid was applied as a standard [17]. Here, 1 mL of extract solution and 1 mL of the standard solution containing different concentrations were taken to the different test tubes. 5 mL diluted FCR and 5 mL solution containing different concentrations of sodium carbonate (7.5 %) were added to each test tube one after another. The test tubes were incubated at 25 °C for 20 min to facilitate the reaction. The test tubes and a blank sample were placed in the UV machine, and absorbance was taken to 760 nm. A standard curve was generated based on the gallic acid, and total phenolic content (TPC) was calculated.

2.4.3. Total flavonoid content test

The crude extract was subjected to measure the total flavonoid content by aluminum chloride colorimetric method using quercetin as standard [18]. 1 mL of extract solution and 1 mL of a standard solution containing different concentrations were taken to the different test tubes. 3 mL methanol, 200 μl aluminum chloride (10 %), 200 μl of 1M potassium acetate, and 5.6 mL of distilled water were added to each test tube one after another. The final mixture was placed in incubation for 30 min to facilitate the reaction. Then, the sample, standard, and blank were placed into UV machine, and absorbance was measured at 420 nm. Total flavonoid content was shown as mg of quercetin equivalent/gm of dried extract.

2.5. In-vitro anti-inflammatory activity

2.5.1. Membrane stabilization activity

The hypotonic solution induced human erythrocyte-lysis model was applied for the membrane-stabilizing activity designed by Shinde et al. [19]. In this screening, 7 mL of venous blood was collected from healthy volunteer by a syringe utilized with EDTA, and then the blood sample was centrifuged by the centrifuged machine at 3000 rpm for 10 min. After that, iso-saline solution was applied to wash blood cells three times and a suspension (10 % v/v) was produced. A 0.5 mL of different concentrations (62.5–1000 μg/mL) of MECR, NFCR, CFCR and diclofenac sodium were taken and 0.5 mL of human Erythrocyte (RBC) suspension, 2 mL of hypotonic saline and 1 mL of phosphate buffer, were mixed and defined as the test solution. The control solution was composed with 0.5 mL of human RBC suspension and hypotonic buffer solution. Then, the mixture was incubated for 30 min at 37°c temperature. After that, the incubated mixture was centrifuged the tubes for 10 min at 3000 rpm. The absorbance of the supernatant solution was measured at 560 nm. Here, diclofenac sodium was applied as a standard agent. The 50 % inhibition concentrations (IC_{50}) value was determined via non-linear inhibition dose-response analysis.

2.5.2. Bovine serum protein denaturation method

The screening of anti-arthritic activity was measured by previously described method [20]. Firstly, 0.05 mL different concentrations (62.5–2000 μg/mL) of crude extracts (MECR, NFCR, CFCR) and Standard solution (Diclofenac sodium) was added to 0.45 mL of BSA (Bovine Serum Albumin, 5 % of w/v aqueous solution), and maintain pH 6.3 by using 1N HCl in all the mixture solutions, and the control solution contained 0.45 mL of BSA solution and 0.05 mL of distilled water. All the mixture solutions were kept for incubation (20 min at a temperature of 37°c), and again retained at 57 °C for half an hour. Then, 2.5 mL of phosphate buffer was added to the

mixture solutions after cooling. Finally, the absorbance of the mixture solutions was measured by using UV spectrophotometer at 416 nm. The non-linear inhibition dose-response analysis method was applied to determine the IC_{50} value of all samples.

2.6. In-vitro cytotoxic activity

2.6.1. Brine shrimp lethality bioassay

The brine shrimp lethality bioassay is subjected to evaluate the cytotoxic properties of crude extracts, and the described method by Mayer et al. was applied for this screening [21]. Here, artificial saltwater (38 g/L) was developed for hatching brine shrimp eggs, to which NaOH (1N) was added to achieve a pH of 8.5, and which was then left at room temperature with a constant supply of oxygen. After 48 h of maturation, the hatched eggs were kept for harvesting shrimp larvae. DMSO (5 mg/mL) mixed with extracts to prepare as a test sample with artificial saltwater. Through serial dilutions, different concentrations (31.25–1000 μg/mL) were established. On the point of positive control, vincristine sulphate was mixed with dilutions to generate different concentrations (0.125–10 μg/mL). Ten live nauplii were put to each experimental vial, which was then kept at room temperature under the light. After the 24 h incubation, the quantity of dead larvae and the mortality rate were counted via a magnifying glass. Vincristine sulphate was used as reference standard treatment.

2.7. Statistical analysis

GraphPad prism version-7.0 software was applied for analyzing the data and preparing the graphs. The data was presented as mean ± SEM, and whereas $^{a}p<0.001$, $^{b}p < 0.01$, $^{c}p < 0.05$ were considered to have statistical significance. One way ANOVA was subjected according to Dunnett's test with comparison to the control. Each experiment was carried out in triplicate and repeated three times for the uniformity of the outcome and statistical function.

2.8. In silico molecular docking

Pattamadilok et al., isolated five compounds from ariel part of *C. rosea* [22]. Those five major phytochemicals were selected and studied through molecular docking to understand their possible molecular interactions with several target proteins mediating anti-oxidant, anti-arthritic, anti-inflammatory, and cytotoxic effects. This experiment was executed in Schrödinger Suite-Maestro v11.1 (Schrödinger LLC, New York, NY, USA).

2.8.1. Preparation of ligand

The structures of selected compounds, namely, beta-sitosterol (PubChem CID:222284), daucosterol (PubChem CID: 5742590), rutin (PubChem CID: 5280805), stigmasterol (CID 5280794), and guanidine (PubChem CID: 3520) were downloaded in SDF format from PubChem database (www.pubchem.ncbi.nlm.nih.gov). The LigPrep tool was employed to prepare these structures in Schrödinger Maestro (v 11.1). Using Epik at pH 7.0 ± 2, possible ionization states were generated, and structures were minimized via the OPLS3 force field.

2.8.2. Preparation of protein

Three-dimensional crystallographic structures of the target proteins were collected from RCSB Protein Data Bank (PDB) (https://www.rcsb.org/) [23]. The enlisted five compounds were tested against human peroxiredoxin 5 (HP-5; PDB ID: 1HD2, 1OC3, 1H4O, and 1URM) [24–26] and catalase (PDB ID: 2CAG) [27] for analyzing antioxidant activity; aggracanase-2 (PDB ID: 3B8Z) [28], matrix metalloproteinase-13 (MMP-13; PDB ID: 5BPA) [29], cyclooxygenase-2 (COX-2; PDB ID: 5F19) [30], hypoxia-inducible factor-2 alpha (HIF-2; PDB ID: 3H7W) [31], and human cathepsin-C (HC-C; PDB ID: 6IC7) [32], for analyzing anti-arthritic activity; COX-2 (PDB ID: 6COX, 1CX2, 5JVY, and 1PXX) [33–35], and cyclooxygenase-1 (COX-1; PDB ID: 3KK6) [36], for analyzing anti-inflammatory activity; epidermal growth factor receptor (EFGF) tyrosine kinase (PDB ID: 1M17 and 2GS7) [37,38], topoisomerase (PDB ID: 3QX3) [39], and endoplasmic reticulum aminopeptidase 2 (ERA-2; PDB ID: 4JBS and 4E36) [40,41] for analyzing cytotoxic activity. The structures of the aforementioned proteins were preprocessed, optimized, and water molecules were removed by using the Protein Preparation Wizard of Schrödinger-Maestro (v11.1). After that, the force field OPLS3 was used to perform the minimization.

2.8.3. Receptor grid generation and molecular docking

The active sites of the prepared proteins were determined by the PockDrug web server [42]. Then a grid was created for each protein, keeping the default parameters of the van der Waals scaling factor and a charge cutoff of 0.25 in glide [43], and it was then subjected to the OPLS3 power field. A bounding box around the active site was set for each protein. The box was set to 14 × 14 × 14 for the docking investigation. Following that, flexible ligand docking was performed using the glide-SP (Glide-Standard Precision) scoring function. Docking analyses were run with the default settings and no ligand-receptor constraints. The best binding affinity for the corresponding protein was found for the ligand with the highest negative docking score.

2.8.4. Ligand-based ADME/T prediction

The absorption, distribution, metabolism, and excretion (ADME) properties of the phytocompounds were projected using the QikProp module embedded in Schrödinger Maestro (v11.1). The oral bioavailability properties of a candidate molecule are determined based on the physicochemical properties postulated in Lipinski's rule of five [44]. Lipinski's rule of five parameters and their

acceptable range are as follows: molecular weight (MW) < 500, number of hydrogen bond acceptors (HB acceptors) ≤ 10, number of hydrogen bond donors (HB donors) ≤ 5, lipophilicity (Log $P_{o/w}$) < 5, and molar refractivity should be between 40 and 130 [45]. Finally, toxicity profiles of the selected compounds such as ames toxicity, carcinogenicity, acute oral toxicity, and rat acute toxicity (LD_{50}, mol/kg) were predicted from the online tool AdmetSAR [46].

2.9. DFT methodology

In this investigation, Five chosen isolated compounds from *C. rosea* were subjected to quantum chemical DFT (density functional test) analysis using the Gaussian 09 software package [47] on a Pentium IV/3.02 Hz (Windows 10.0 with 4 GB of RAM) platform via Gauss View 6.0.10 molecular visualization software [48]. On the basis of the optimized structure, the electronic characteristics, including point group, energy value of HOMO (EHOMO), molecule electrostatic potential, energy value of LUMO (ELUMO), global reactivity descriptors & HOMO-LUMO energy gap were calculated in gas phase. Density Functional Theory (DFT) measurements were conducted in full utilizing the Becke's three parameter hybrid exchange functional [49] and the Lee-Yang-Parr correlation functional (B3LYP) [50,51] at the 6-31G+ (d, p) level of theory [52].

3. Results

3.1. Preliminary phytochemical screening

The qualitative phytochemical screening of MECR manifested the existence of carbohydrates, alkaloids, tannins, reducing sugar, phenols, flavonoids, and saponins (Table 1).

3.2. In-vitro antioxidant assay

3.2.1. Ferric-reducing power capacity (FRPC)

Any possible antioxidants with an affinity for electron-transfer function, acts as a sign of reduction in the power of a compound. As in Fig. 1 were summarized the reducing power activity of all crude extracts and the orders were as followed: ascorbic acid > MECR > NFCR > CFCR. Among all extractives, MECR showed the maximum reducing power capacity (2.49) at 1000 μg/mL concentration, whereas the standard ascorbic acid exhibited the maximum absorbance (3.29) at the same concentration on the spectrophotometer measurement.

3.2.2. Total phenolic and flavonoid content test

The total phenol and flavonoid content of the different fractions of *C. rosea* were estimated quantitatively and the result is displayed in Table 2. The phenolic potentials of MECR, NFCR and CRCR were found 200.51 ± 2.09, 154.70 ± 1.86 and 169.65 ± 1.32 mg GAE/gm respectively. The maximum flavonoid content was found in n-hexane fraction of *C. rosea* (NFCR) that is 60.33 ± 0.73 mg QE/gm, and MECR and CFCR were found 52.19 ± 0.70 and 48.69 ± 1.07 QE/gm. Here, the plant extract was carried out through linear regression equation (for flavonoid activity, equation stands as $y = 0.0102\times - 0.0637$; for phenol assay, it was $y = 0.0039x + 0.033$).

3.3. In vitro anti-inflammatory activity

3.3.1. Membrane stabilization activity

In this investigation, the inhibition of hemolysis of methanol extracts of *C. rosea* (MECR) and its different organic soluble fractions (NFCR & CFCR) were found dose-dependent and significantly protected lysis of human erythrocyte membrane induced by hypotonic solution (Fig. 2, S1 and S3). The maximum percentage of inhibition of MECR, NFCR and CFCR were 73.91 % ± 1.45 %, 74.85 % ± 0.57 % and 67.35 % ± 4.04 % at 1000 μg/mL concentration respectively. Moreover, standard Diclofenac sodium showed the maximum percentage of inhibition (85.35 % ± 2.11 %) at 1000 μg/mL concentration. In-addition, MECR and CFCR showed better

Table 1
Result of the phytochemical screening of methanol extract of *C. rosea* leaves (MECR).

Phytochemicals	Appearance	Results
Carbohydrates	Molisch's test: reddish color ring form	+
Tannins	FeCl3 test: a brownish green color form	+
Alkaloids	Wagner test: A reddish brown color	+
	Mayer's test: Yellow color form	+
Reducing sugar	Fehling's test: red precipitate form	+
Phenols	$FeCl_3$ test: violet color form	++
Flavonoids	Lead acetate test: a fluorescence yellow color form	+
Saponins	Froth test: Persistent forth for 1 h	++
Glycosides	Shinoda test: no deep red color form	–
Proteins	No violet color form	–

Here, ++: Highly present; +: moderately present; −: absent.

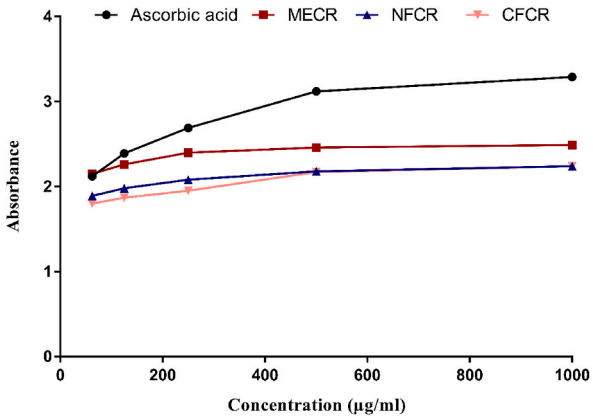

Fig. 1. Reducing power capacity of MECR, NFCR and CFCR extract of *C. rosea,* compared with ascorbic acid, reducing capacity vs. concentration.

Table 2
Total phenol and flavonoid contents of *C. rosea* fractions.

Chemical/Plant extract	Total Phenol Content (mg GAE/g dried extract)	Total Flavonoid Content (mg QE/g dried extract)
MECR	200.51 ± 2.09	52.19 ± 0.70
NFCR	154.70 ± 1.86	60.33 ± 0.73
CFCR	169.65 ± 1.32	48.69 ± 1.07

MECR: methanol extract of *C. rosea* leaves, NFCR: n-hexane fraction of *C. rosea* leaves, and CFCR: Chloroform fraction of *C. rosea* leaves.

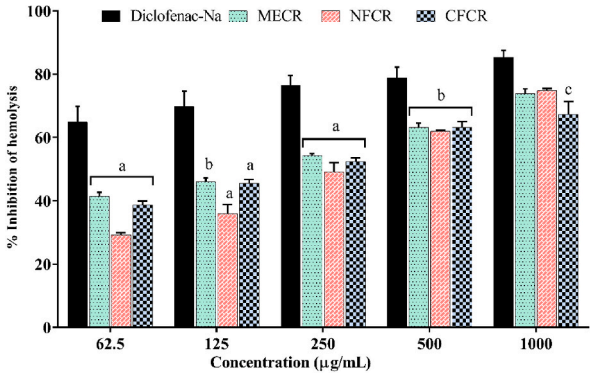

Fig. 2. Percentage of hemolysis inhibition of MECR, HFCR and CFCR extract of *C. rosea,* with compare to standard diclofenac sodium. [a] $p < 0.001$ compared with reference standard drug Diclofenac Sodium (Dunnett's test). Each value expressed in the figure as mean ± SEM (n = 3).

efficacy with IC_{50} were 64.63 and 59.58 µg/mL. The standard drug possessed highest inhibition with IC50 is 20.57 µg/mL.

3.3.2. Bovine serum protein denaturation inhibition

The anti-arthritis potentiality of *C. rosea* leaves was exhibited on Fig. 3, S2 and S3. All the of crude extractives (MECR, NFCR and CFCR) were manifested dose-depending and significantly inhibitory properties on protein denaturation assay, in which MECR, NFCR and CFCR manifested strongly significant ($p<0.001$) inhibitory potency at 500 µg/mL & 1000 µg/mL concentration. The peak inhibitory properties of MECR, NFCR and CFCR were found 67.54 % ± 1.85 %, 79.41 % ± 1.30 % and 72.14 % ± 1.15 % at 2000 µg/mL concentrations respectively, whereas standard diclofenac sodium showed 94.11 % ± 2.00 % inhibition properties at same concentrations. Notably, NFCR showed highest inhibition potency among other plant extract with IC_{50} value is 28.72 µg/mL that was very similar to standard diclofenac sodium (18.95 µg/mL). The IC50 of MECR and CFCR were 76.14 and 110.6 µg/mL.

3.4. In-vitro cytotoxic activity

3.4.1. Brine shrimp lethality bioassay

Fig. 4 and S4, summarized the lethality concentration (LC_{50}) values with the linear regression equation and the mortality rate of MECR, NFCR and CFCR. In this screening, all the crude extracts manifested moderate toxic, and the mortality rate of MECR, NFCR and

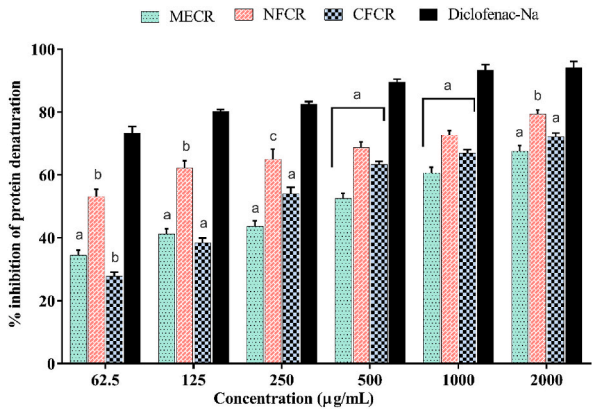

Fig. 3. Percentage of protein inhibition of MECR, NFCR and CFCR extract of *C. rosea,* with compare to standard Diclofenac sodium. Values are represented as mean ± SEM (n = 3); [a] $p < 0.001$ is statistically significant comparison with diclofenac sodium followed by Dunnett's test.

CFCR are 169.05, 149.43 and 123.54 µg/mL, respectively. The positive control vincristine sulphate exhibited the LC_{50} value at 2.16 µg/mL concentration.

3.5. *In silico molecular docking*

The docking scores and glide energies of the phytochemicals that were previously identified in the C. *rosea* against the proteins involved in oxidative stress, arthritis, inflammation, and cancer have been displayed in Tables 3–6. The interactions of the compounds with respective target proteins associated with antioxidants, anti-arthritic, anti-inflammatory, antioxidant, and cytotoxic activities have been illustrated in Figs. 5–8.

Table 3 & Fig. 5(**a–e**)**,** shows the docking scores of daucosterol (Fig. 5d), guanidine (Fig. 5b), rutin (Fig. 5c), stigmasterol (Fig. 5e), and beta-sitosterol (Fig. 5a) against HP-5 and catalase for antioxidant effect. Among the compounds, rutin manifested the highest docking scores of −4.445, −5.668, −6.186, and −4.976 kcal/mol against all of the HP-5 proteins, specifically, 1HD2, 10C3, 1H4O, and 1URM (Fig. 5c), respectively, compared to the reference standard antioxidant ascorbic acid, indicating that it possesses favorable binding affinity at the active site of the respective protein. Besides, it also showed the maximum docking scores (−7.52 kcal/mol) amongst the studied compounds against catalase (PDB ID: 2CAG).

Table 4 & Fig. 6(**a–e**)**,** represents the results of the molecular docking study of C. *rosea* compounds for anti-inflammatory activity. In the case of COX-2 (PDB ID: 6COX), rutin showed the best docking score of −6.298 kcal/mol, followed by daucosterol and guanidine. The docking scores of the latter compounds were assessed to be −3.728 and −3.702 kcal/mol. With regards to the other COX-2 proteins (PDB ID: 5JVY and 1CX2), the binding strength of rutin was found to be significantly higher than the standard anti-inflammatory agent aspirin. Rutin showed docking sores of −6.901 kcal/mol and −8.78 kcal/mol (Fig. 6a), respectively, against those proteins, in contrast to the −5.834 and −6.243 kcal/mol docking scores of aspirin. Daucosterol and stigmasterol also possessed favorable binding affinity against PDB ID: 5JVY with docking scores of −4.985 kcal/mol (Fig. 6c) and −4.965 kcal/mol, respectively. However, on the other hand, only Guanidine showed binding affinity against PDB ID: 1PXX (Fig. 6b) among the studied compounds.

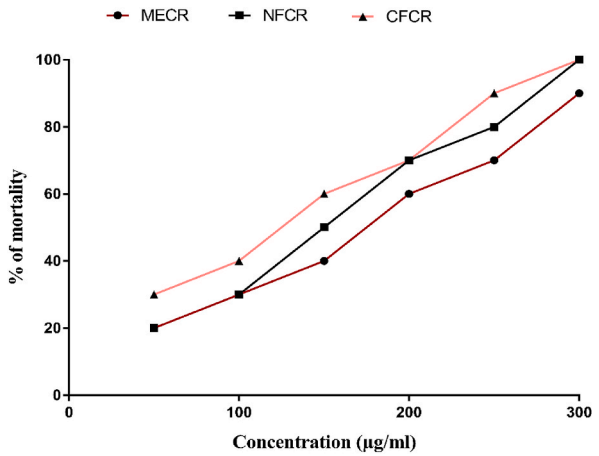

Fig. 4. The mortality rate of brine shrimp nauplii of vincristine sulphate and different extract fraction concentrations.

Table 3
Docking score for anti-oxidant activity.

Ligand	Proteins									
	Anti-oxidant activity									
	1HD2		1OC3		2CAG		1H4O		1URM	
	DS	GE	DS	GE	DS	GE	DS	GE	DS	GE
Ascorbic acid	−5.751	−25.43	−6.964	−32.65	−7.692	−29.45	−6.942	−30.70	−5.98	−27.75
Daucosterol	−3.188	−31.13	−3.084	−27.76	−3.726	−38.25	−3.017	−27.11	−2.4	−27.20
Guanidine	−4.142	−8.29	−3.247	−8.29	−3.959	−8.25	−3.792	−7.31	−4.01	−8.49
Rutin	−4.445	−48.40	−5.668	−52.38	−7.52	−29.45	−6.186	−57.32	−4.97	−49.51
Stigmasterol	−2.324	−22.30	−3.286	−25.12	−4.48	−27.14	−3.954	−30.43	−2.45	−22.01
Beta sitosterol	−2.074	−21.60	−3.117	−24.06	−3.749	−24.81	−3.286	−25.11	−1.80	−20.36

DS = Docking score, GE = Glide energy.

Table 4
Docking score for anti-inflammatory activity.

Ligand	Proteins									
	Anti-inflammatory activity									
	6COX		5JVY		1CX2		3KK6		1PXX	
	DS	GE	DS	GE	DS	GE	DS	GE	DS	GE
Aspirin	−8.996	−38.99	−5.834	−33.49	−6.243	−26.75	−5.794	−22.56	−7.483	−30.43
Daucosterol	−3.728	−40.64	−4.985	−49.77	–	–	–	–	–	–
Guanidine	−3.702	−9.018	−3.737	−10.85	−4.08	−10.92	−3.965	−10.27	−3.311	−6.85
Rutin	−6.298	−71.80	−6.901	−59.11	−8.78	−75.56	−6.901	−59.19	–	–
Stigmasterol	−3.205	−28.68	−4.965	−30.40	–	–	–	–	–	–
Beta sitosterol	−2.336	−23.23	−2.582	−17.72	–	–	–	–	–	–

DS = Docking score, GE = Glide energy.

Table 5
Docking score for anti-arthritic activity.

Ligand	Proteins									
	Anti-arthritic activity									
	3B8Z		5BPA		5F19		3H7W		6IC7	
	DS	GE	DS	GE	DS	GE	DS	GE	DS	GE
Diclofenac sodium	−8.075	−34.53	−6.141	−36.76	−3.932	−32.22	−7.809	−35.47	−4.771	−34.94
Daucosterol	−5.044	−50.47	−4.980	−22.88	−4.47	−33.15	–	–	−4.634	−48.78
Guanidine	−4.582	−13.17	−3.939	−10.72	−3.528	−8.26	−4.041	−10.99	−3.939	−10.72
Rutin	−7.618	−67.96	−8.297	−70.21	−6.161	−63.24	–	–	−7.677	−70.78
Stigmasterol	−4.285	−39.01	−4.788	−31.39	−3.704	−23.00	–	–	−3.007	−26.91
Beta sitosterol	−4.171	−39.15	−5.356	−34.13	−3.678	−10.01	–	–	−3.678	−10.01

DS = Docking score, GE = Glide energy.

Table 6
Docking score for cytotoxic activity.

Ligand	Proteins									
	Cytotoxic activity									
	1M17		3QX3		2GS7		4JBS		4E36	
	DS	GE	DS	GE	DS	GE	DS	GE	DS	GE
Doxorubicin	−8.837	−62.70	−9.52	−64.16	−6.514	−60.93	−6.815	−66.64	−3.506	−44.01
Daucosterol	−4.577	−44.19	−8.429	−49.61	−4.555	−48.04	−5.188	−54.71	–	–
Guanidine	−4.831	−11.69	−4.627	−10.96	−3.866	−8.53	−4.768	−13.29	−5.767	−12.99
Rutin	−8.876	−74.39	−10.569	−82.85	−7.173	−86.46	−9.627	−87.74	−6.95	−59.31
Stigmasterol	−3.481	−31.61	−7.419	−39.31	−3.5	−34.24	−5.321	−37.92	−2.667	−25.71
Beta sitosterol	−3.722	−28.33	−5.633	−35.17	−3.482	−34.61	−4.949	−36.97	−2.602	−25.35

DS = Docking score, GE = Glide energy.

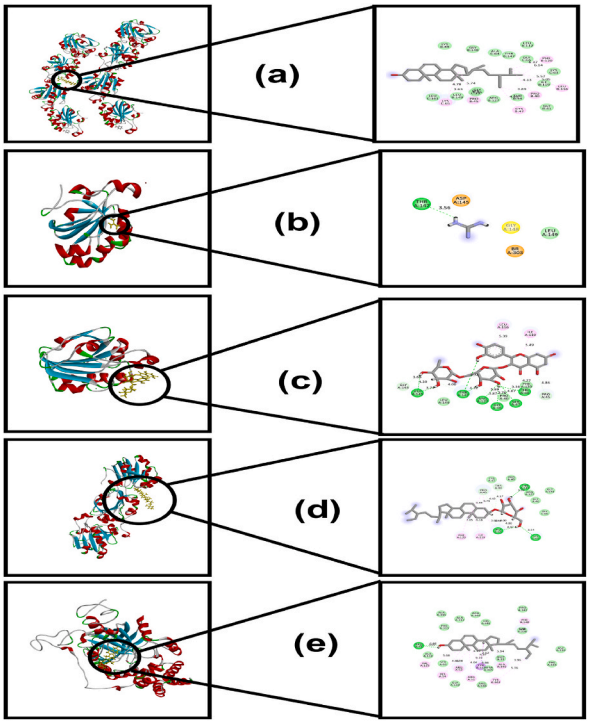

Fig. 5. a. Interaction of Beta-Sitosterol with HP-5 (PDB id: 1H4O); b. Interaction of Guanidine with HP-5 (PDB id: 1HD2); c. Interaction of Rutin with HP-5 (PDB id: 1URM); d. Interaction of Daucosterol with HP-5 (PDB id: 1OC3); e. Interaction of Stigmasterol with catalase (PDB id: 2CAG).

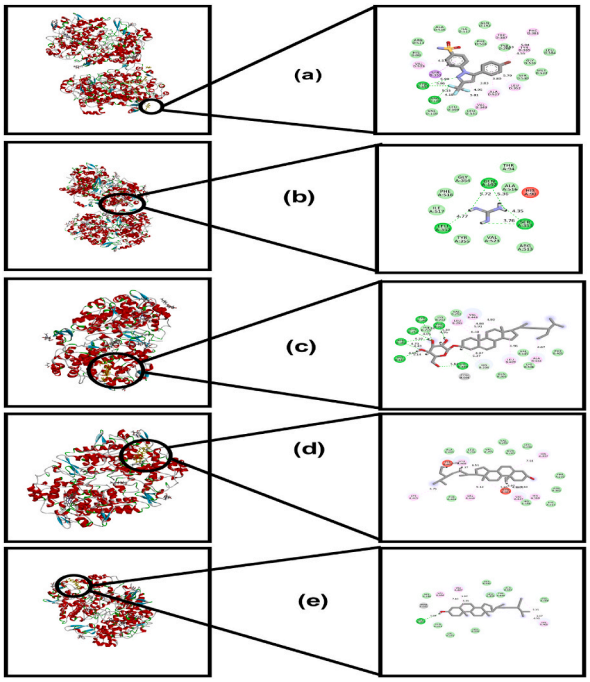

Fig. 6. a. Interaction of Rutin with COX-2 (PDB id: 1CX2); b. Interaction of Guanidine with COX-2 (PDB id: 1PXX); c. Interaction of Daucosterol with COX-2 (PDB id: 5JVY); d. Interaction of Stigmasterol with COX-2 (PDB id: 6COX); e. Interaction of Beta-Sitosterol with COX-2 (PDB id: 6COX).

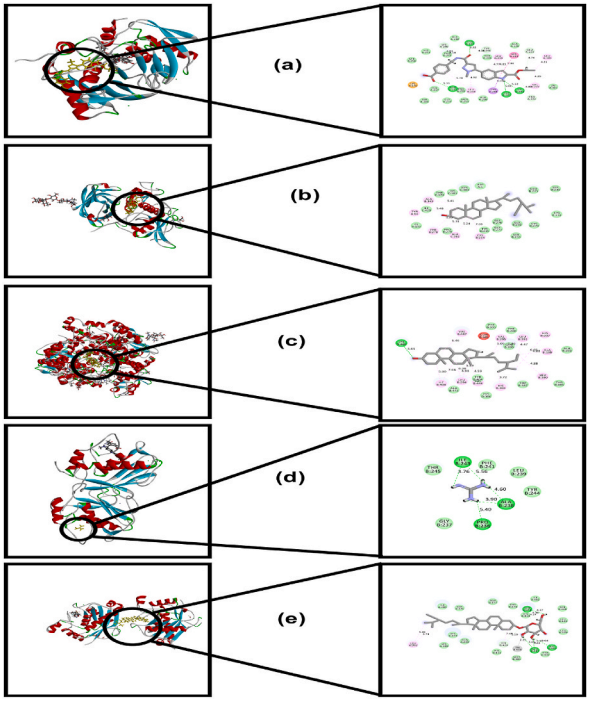

Fig. 7. a. Interaction of Rutin with MMP-13 (PDB id: 5BPA); b. Interaction of Beta-Sitosterol with HC-C (PDB id: 6IC7); c. Interaction of Stigmasterol with COX-2 (PDB id: 5F19); d. Interaction of Guanidine with MMP-13 (PDB id: 5BPA); e. Interaction of Daucosterol with aggracanase (PDB id: 3B8Z).

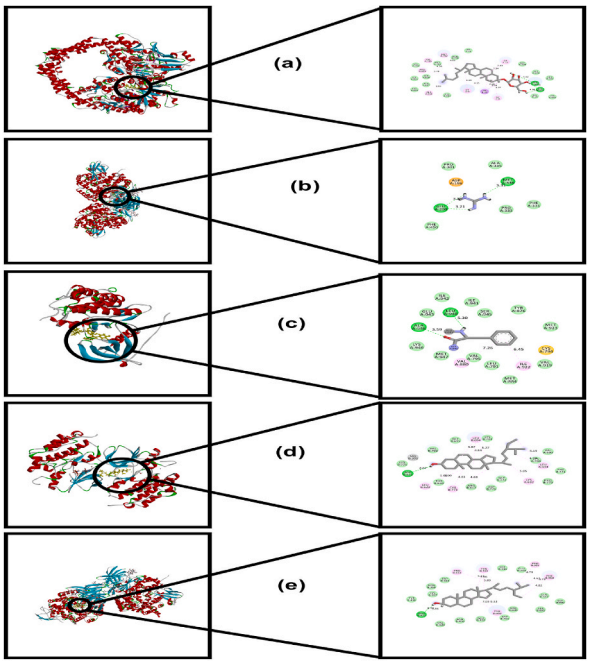

Fig. 8. a. Interaction of Daucosterol with topoisomerase (PDB id: 3QX3); b. Interaction of Guanidine with ERA-2 (PDB id: 4E36); c. Interaction of Rutin with EGFR kinase (PDB id: 1M17); d. Interaction of Stigmasterol with EGFR kinase (PDB id: 2GS7); e. Interaction of Beta-Sitosterol with ERA-2 (PDB id: 4JBS).

Nonetheless, rutin further manifested a higher docking score (−6.901 kcal/mol) against COX-1 (PDB ID: 3KK6) compared to aspirin (docking score: −5.794 kcal/mol).

The findings of the molecular docking study for anti-arthritic activities have been listed in Table 5 & Fig. 7**(a–e)**. Analysis of the docking scores revealed that rutin (docking score: −7.618 kcal/mol) possesses the highest binding affinity against 3B8Z, followed by daucosterol (docking score: −5.044 kcal/mol) and guanidine (−4.582 kcal/mol). In the cases of MMP-13 (PDB ID: 5BPA) and COX-2 (PDB ID: 5F19), the docking scores of rutin were found to be −8.297 (Fig. 7a) and −6.161 kcal/mol, which is higher compared to the docking scores of the reference anti-arthritic agent diclofenac sodium. Among the compounds, only guanidine showed binding energetics against HIF-2 (PDB ID: 3H7W) with a docking score of −4.041 kcal/mol. On the other hand, both rutin and guanidine showed favorable binding affinity against HC-C (PDB ID: 6IC7) with docking scores of −7.677 and −4.634 kcal/mol, respectively, when compared to the docking scores of diclofenac.

The docking study for cytotoxic activity (Table 6 & Fig. 8a–e) was carried out with the following targets in mind: EFGF tyrosine kinase (PDB ID: 1M17 and 2GS7), topoisomerase (PDB ID: 3QX3), and ERA-2 (PDB ID: 4JBS and 4E36). The highest binding energy against both proteins of the EFGF tyrosine kinase was assessed for rutin. Rutin showed docking scores of −8.876 and −7.173 kcal/mol against 1M17 (Fig. 8c) and 2GS7, respectively, which are comparatively higher than the docking scores of the reference standard anticancer drug doxorubicin. Rutin also demonstrated maximum docking scores of −10.569 kcal/mol against topoisomerase (PDB ID: 3QX3), followed by daucosterol (docking score: −8.429 kcal/mol) (Fig. 8a) and stigmasterol (docking score: −7.419 kcal/mol). In the case of ERA-2 (PDB ID: 4JBS and 4E36), the docking scores of rutin were estimated to be −9.627 and −6.95 kcal/mol, higher than the docking scores manifested by doxorubicin (docking scores: −6.815 and −3.506 kcal/mol, respectively). Guanidine also manifested better affinity against the active site residues of PDB ID: 4E36 compared to doxorubicin, with a docking score of −5.767 kcal/mol (Fig. 8b).

Additionally, we have looked into the potential pharmacological effects of a few phytocompounds using the structure-based biological activity prediction tool "Prediction of activity spectra for substances" in order to support the findings of our laboratory experiments (PASS). In order for a molecule to be regarded pharmacologically prospective, the value of probable activity (Pa) must be greater than the value of likely inactivity (Pi) (Table 7). Here, agents are recognized as pharmacological potential which manifest Pa value 0.7. However, the predicted biological activities of all of the chosen phytocompounds were in agreement with our laboratory investigations; in particular, the Pa values of Rutin, Beta-Sitosterol, methyl, and Daucosterol were more promising, indicating that the compounds of *C. rosea* have likely pharmacological potentials and may be targets against particular receptors.

3.6. ADME/T properties

Tables 8 and 9, represent the predicted pharmacokinetics and toxicological properties of the compounds found in C. *rosea*. The possible oral bioavailability of the compounds was predicted considering the physicochemical parameters mentioned in Lipinski's rules of five. According to our findings, the number of Lipinski's violations of the analyzed compounds was between 0 and 4; whereas beta-sitosterol, daucosterol, and stigmasterol violated two of Lipinski's rules, rutin violated four of Lipinski's rules, and guanidine did not violate any of Lipinski's rules. The findings of the toxicological analysis showed that all the compounds are expected to possess negative ames toxicity and carcinogenicity profiles. The acute oral toxicity values of beta-sitosterol and stigmasterol were ascertained

Table 7
Biological activity prediction of selective isolated compounds of *Canavalia rosea* by (PASS) online.

SN	Compound	Activity	Pa	Pi
1	Daucosterol	Immunosuppressant	0.793	0.005
		Antiviral (Influenza)	0.767	0.003
		Antitoxic	0.762	0.004
		Antifungal	0.722	0.009
		Antioxidant	0.340	0.018
		Anti-inflammatory	0.621	0.028
		Antineoplastic	0.630	0.039
2	Rutin	Anti-inflammatory	0.728	0.013
		Antibacterial	0.677	0.005
		Antidiabetic	0.528	0.019
		Anti-hypoxic	0.498	0.038
		Antileukemic	0.450	0.019
3	Stigmasterol	Anti-hypercholesterolemic	0.970	0.002
		Antinociceptive	0.601	0.008
		Anti-inflammatory	0.542	0.045
		Antineoplastic	0.553	0.056
		Antifungal	0.490	0.032
4	Beta-Sitosterol	Immunosuppressant	0.762	0.009
		Bone diseases treatment	0.718	0.005
		Antineoplastic (endocrine cancer)	0.173	0.080
		Antiviral (Influenza)	0.686	0.006
		Antifungal	0.585	0.020
		Anti-inflammatory	0.467	0.067

Table 8
ADME properties of selective isolated compounds of *Canavalia rosea* using swiss ADME/T online tool.

SN	Compound name	MW(g/ml)	HB Acceptor	HB Donor	Log $P_{o/w}$	Molar refractivity	Violation
1	Daucosterol	576.85	6	4	5.15	165.61	2
2	Guanidine	59.07	1	3	−1.01	15.93	0
3	Rutin	610.52	16	10	−1.12	141.38	4
4	Stigmasterol	412.69	1	1	6.96	132.75	2
5	β-Sitosterol	414.71	1	1	7.19	133.23	2

Serial number (SN); Molecular weight (MW) - (acceptable range: <500); Hydrogen bond acceptor (HB acceptor) - (Acceptable range: ≤10); Hydrogen bond donor (HB donor) - (Acceptable range: ≤5); Lipophilicity (Log $P_{o/w}$) - (acceptable range<5); Molar refractivity should be between 40 and 130. Rule of five: Number of violations of Lipinski's rule of five: accepted range: 0–4.

Table 9
Toxicological properties of selective isolated compounds of *C. rosea* using admetSAR online tool.

SN	Compound	Ames Toxicity	Carcinogens	Acute Oral Toxicity	Rat Acute Toxicity (LD 50, mol/kg)
1	Daucosterol	Non AMES toxic	Non-carcinogens	III	2.9113
2	Guanidine	Non AMES toxic	Non-carcinogens	II	1.9367
3	Rutin	Non AMES toxic	Non-carcinogens	III	2.4948
4	Stigmasterol	Non AMES toxic	Non-carcinogens	I	2.6561
5	Beta-Sitosterol	Non AMES toxic	Non-carcinogens	I	2.6561

to fall into "Category-I" (LD_{50} values less than or equal to 50 mg/kg). In contrast, the acute oral toxicity value of guanidine falls into "Category-II" (50 mg/kg < LD_{50} < 500 mg/kg), while the acute oral toxicity value of guanidine falls into daucosterol and rutin "Category-III" (500 mg/kg < LD_{50} < 5000 mg/kg). Besides, most compounds displayed weak acute toxicity in rats with an LD_{50} value ranging from 1.9367 to 2.9113 mol/kg, indicating that they possess a riskless acute oral toxicity profile.

3.7. Structural optimization

The DFT/B3LYP/6-31+G (d, p) level calculations of the optimized molecular structures of five distinct isolated compounds from *C. rosea* were provided in Table 10 & Fig. 9(A–E). All isolated compounds fall belong to the C1 point group symmetry from a structural optimization perspective. The selective five compounds manifested dipole moments of 13.699, 2.029, 1.855, 2.032 and 3.428 debye for Rutin, Daucosterol, β-Sitosterol, Stigmasterol, Guanidine respectively. The molecular optimization energies for Rutin (Fig. 9C), Daucosterol (Fig. 9A), β-Sitosterol (Fig. 9E), Stigmasterol (Fig. 9D) and Guanidine (Fig. 9B) are −2249.72478 a.u, −1820.66941 a.u, −1210.12708 a.u, −1208.90594 a.u, and −205.29984 a.u, respectively.

3.8. Molecular electrostatic potential (MESP)

The molecular electrostatic potential (MESP) map [53] with surface contours had been depicted using Gauss view 6.0.10 computer software at 0.005 isosurface value. Different values are used to represent the various colors of the MESP map. The MESP surface has a color scheme that includes red, which is electron rich with partially negative charge; yellow, which is slightly electron rich; green, which is neutral; blue, which is electron deficient with partially positive charge; and light blue, which is slightly electron deficient, all of which are suitable for nucleophilic attack. The potential values for the specified isolated compounds such as Rutin, Daucosterol, β-Sitosterol, Stigmasterol and Guanidine range from $-8.481e^{-2}$ a.u to $+8.481e^{-2}$ a.u (Fig. 10C), $-6.995e^{-2}$ a.u to $+6.995e^{-2}$ a.u (Fig. 10A), $-6.100e^{-2}$ a.u to $+6.100e^{-2}$ a.u (Fig. 10E), $-6.340e^{-2}$ a.u to $+6.340e^{-2}$ a.u (Fig. 10D), and $-7.382e^{-2}$ a.u to $+7.382e^{-2}$ a.u (Fig. 10B) respectively were given in Fig. 10. All of the isolated compounds that were chosen are suitable for electrophilic and nucleophilic reactions both. Moreover, all of the isolated compounds that were identified have O and H atom regions, which are most likely engaged in the electrophilic and nucleophilic reactions, respectively.

Table 10
Optimized molecular energy of five selective isolated compounds with dipole moment.

Compounds	Point group	Energy (a.u)	Dipole moment (Debye)
Daucosterol	C1	−1820.66941	2.029
Guanidine	C1	−205.29984	3.428
Rutin	C1	−2249.72478	13.699
Stigmasterol	C1	−1208.90594	2.302
Beta sitosterol	C1	−1210.12708	1.855

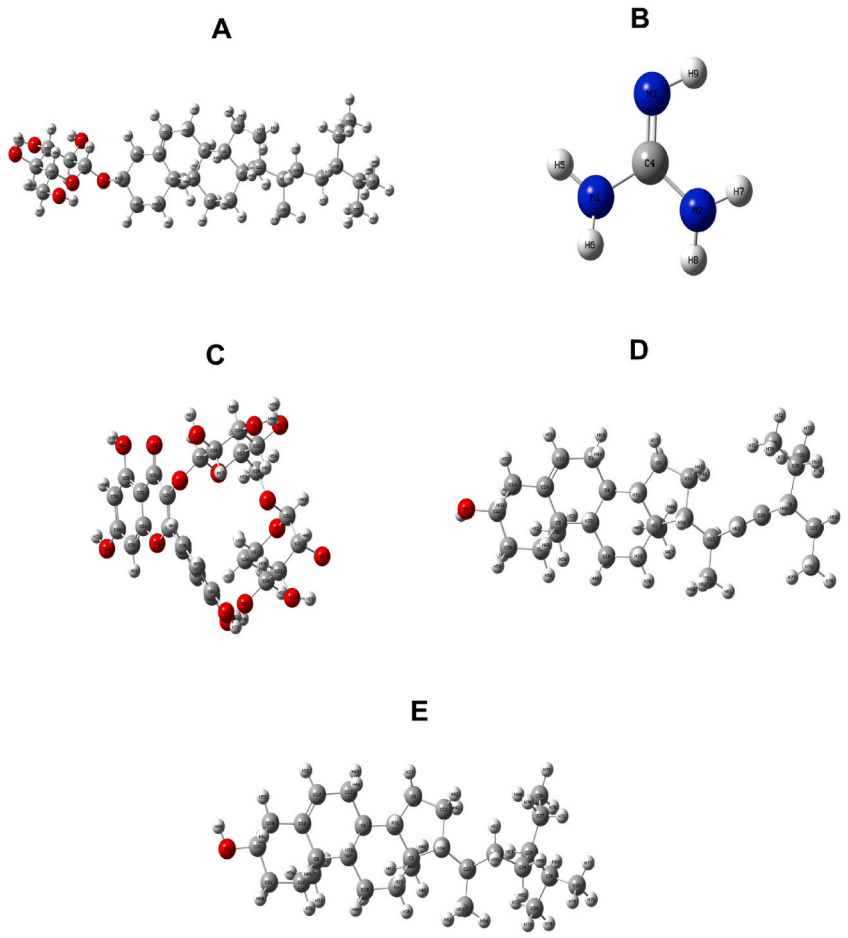

Fig. 9. Optimized geometric structures with numbering of atoms of five selected isolated compounds A. Daucosterol B. Guanidine C. Rutin D. Stigmasterol E. Beta sitosterol.

3.9. FMOs and global descriptors

The highest occupied molecular orbital (HOMO), which resembles a valence band, and the lowest unoccupied molecular orbital (LUMO), which resembles a conduction band, are sometimes referred to as frontier molecular orbitals (FMOs), had shown in Table 11 & Fig. 11 which measured at the DFT/B3LYP/6-31G+ (d, p) level for Rutin (Fig. 11C), Daucosterol (Fig. 11A), β-Sitosterol (Fig. 11E), Stigmasterol (Fig. 11D) and Guanidine (Fig. 11B), respectively. Rutin displays the lowest energy gap among the five isolated compounds that were selected, indicating that it is more reactive than the others (Fig. 11C). However, guanidine has the biggest energy gap value, which implies that it is a hard molecule (Fig. 11B). The chemical reactivity order of five selected isolated compound is- Rutin > Daucosterol > Stigmasterol > β-Sitosterol > Guanidine.

4. Discussion

In the era of civilization, natural products exhibited a meaningful source of potentiality for the establishment of new therapeutic approach that are derived from medicinal plants [54]. However, pharmacologist and researcher have faith that herbal medicines are the promising source of numerous biomolecules, which have multifaceted pharmacological targets. Thus, those agents provided a novel mechanistic pathway having a wide range of biological activity (e.g. anti-inflammatory, antioxidant, thrombolytic, anti-arthritic, etc.) that led to the development of the treatment of several kinds of diseases [55]. In recent history, 30 % of pharmaceuticals are synthesized from natural plants & the number is increasing day by day due to the significant value of medicinal plants [56]. In our study, phytochemical screening of the methanol extract of *C. rosea* leaves (MECR) confirmed the presence of a wide range of chemical entities which can be associated with several pharmacological activities given by the plant extract.

A large number of chemical reactions occurred in our human body and produced free radicals which led to oxidative stress in the catabolism and anabolism process. Cellular damage, aging, cancer, inflammation, rheumatic arthritis and several cardiovascular diseases were induced by excess generation of free radicals [57,58]. Thus, antioxidants are vital elements that play a magnificent role

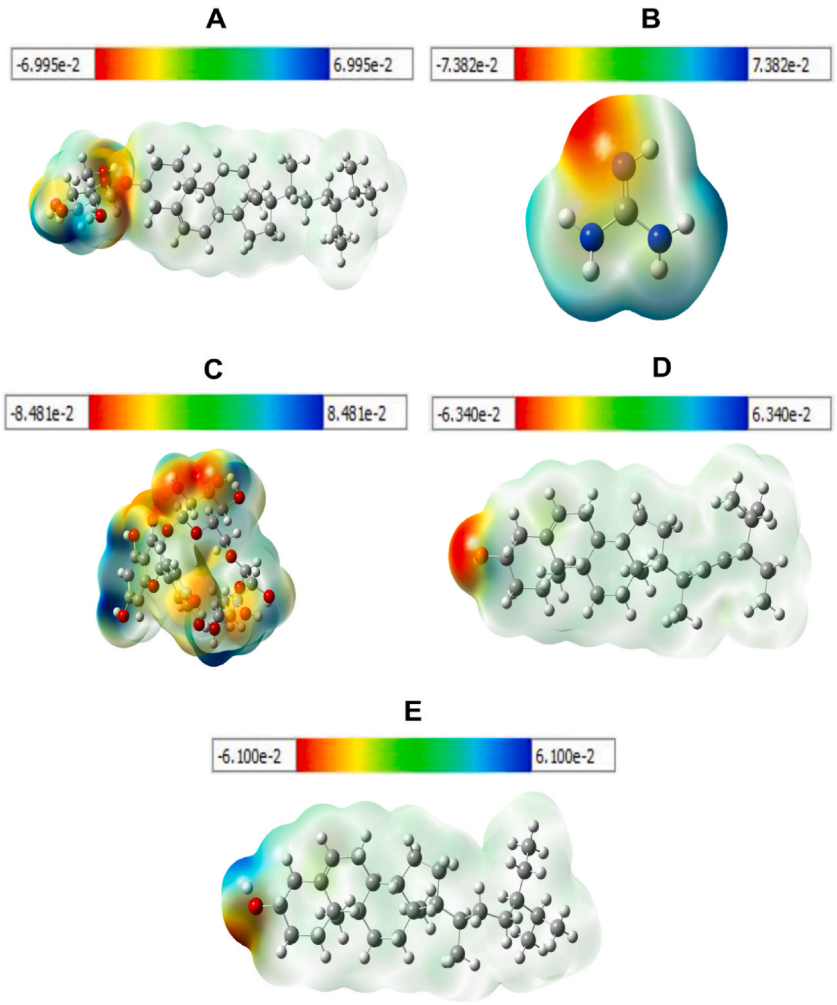

Fig. 10. Molecular electrostatic potential surface for five selected isolated compounds in (a.u); the electron density isosurface being 0.0004 (a.u) A. Daucosterol B. Guanidine C. Rutin D. Stigmasterol E. Beta sitosterol.

Table 11
Global reactivity descriptor values of five selective isolated compounds.

Derivatives	IP (eV)	EA (eV)	H	S	μ	χ	ώ
Daucosterol	6.24692	0.69090	2.77801	0.35997	−3.46891	3.46891	6.01667
Guanidine	5.77290	−1.73636	3.75463	0.26634	−2.01827	2.01827	2.03671
Rutin	5.32690	1.53363	1.89663	0.52725	−3.43027	3.43027	5.88337
Stigmasterol	6.20229	−0.69770	3.45000	0.28986	−2.75230	2.75230	3.78757
Beta sitosterol	6.20202	−0.76001	3.48102	0.28727	−2.72100	2.72100	3.70193

[IP = Ionization potential, EA = Electron affinity, η = Global hardness, S = Global softness, μ = Chemical potential, χ = Electronegativity, ω = Electrophilicity index].

in mitigating damage caused by oxidative stress [59]. As a natural reservoir, plants are manifested an excellent source of antioxidants such as polyphenolic substances (e.g. flavonoid, phenolic acids, etc.) [60]. In our investigation, an UV spectrometric analysis of MECR, NFCR and CFCR demonstrated a significant decrease of the quantity of radical scavenging on ferric reduction assay as 2.49, 2.24 and 2.24 at 1000 μg/mL concentration respectively, which were partially close to reference standard ascorbic acid with (3.29) at the same concentration. In-addition, the quantitative analysis showed potential anti-oxidant potentiality in Total phenolic and flavonoid content assay.

Inflammation is a normal action to tissue damage & a complicated enzymatic reaction scheme [61]. The membrane of erythrocytes (RBCs), is regarded as being comparable to the cellular lysosomal membrane and the strength of erythrocytes depends on the integrity of their membrane, whereas exposure of erythrocytes to the hypotonic solution medium leads to lysis of membrane and causing further

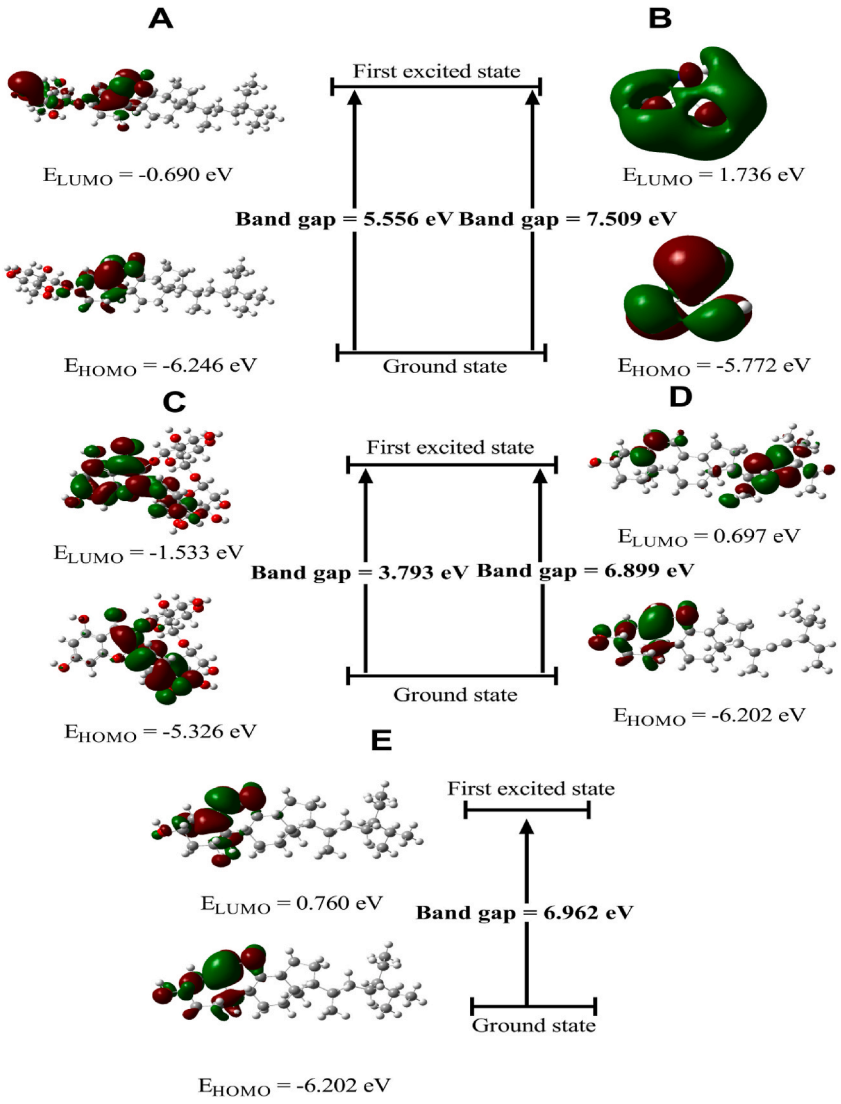

Fig. 11. HOMO-LUMO band gap for five selected isolated compounds A. Daucosterol B. Guanidine C. Rutin D. Stigmasterol E. Beta sitosterol.

tissue damage or inflammation [62]. Numerous physiochemical factors (e.g., burns, heat, hypotonic solutions, drugs, etc.) play their progressive role to rupture of the erythrocytes membrane and generated plenty of disorders. Therefore, the lysosomal membrane has to be stabilized to overcome the pathogenesis of inflammation, which is a model method for investigating ant-inflammatory activity [63]. In this anti-inflammatory inquiry, the result of all extractives demonstrated significantly inhibition of hypotonic solution-induced hemolysis with a comparison of the reference standard drug Diclofenac sodium. Also, MECR and CFCR were exhibited partially equal value whereas NFCR was manifested minimum inhibition among all concentrations. In addition, free radical scavenger like phenolic compounds may also exerts anti-inflammatory properties by membrane stabilization mechanism that enriches the potentiality of this plant [64].

Denaturation of protein produce auto-antigen which are responsible for arthritic diseases as well as inflammatory response, and the modification of hydrophobic, hydrogen, disulfide, and electrostatic bonds may be a contributing factor in this protein denaturation process [65]. However, the main mechanism scheme of non-steroidal anti-inflammatory drugs (NSAIDs) which discovered before manifested the protection against protein denaturation by their inhibitory effect on cyclooxygenase, may play a vital role in the management of arthritis and anti-inflammation [66,67]. In our recent assessment, all organic soluble fraction manifested significantly obstruction of protein denaturation. In addition, MECR, NFCR and CFCR showed strongly significant ($p < 0.001$) inhibitory potency at both 500 μg/mL & 1000 μg/mL concentration.

The toxicity properties of plant materials is a crucial concern to the researcher in the time of the development of new therapeutic entity [68]. The brine shrimp lethality bioassay has been a substantiated system to evaluate the safe biological safe products [69]. This study can show the relationship between natural plant extract and biological reaction as well as also help to maintain the

administration dose development scheme of animal models [70]. In this study, the toxicity properties were calculated as strong when the ranged $0 < LC_{50} < 100$ μg/mL; moderate when the ranged $100 \leq LC_{50} \leq 500$ μg/mL, weak when ranged from $500 \leq LC_{50} \leq 1000$ μg/mL and ranged from $LC_{50} \geq 1000$ μg/mL were considered as non-toxic [71]. Therefore, MECR, NFCR and CFCR exhibited dose-dependent toxicity with LC_{50} 169.05, 149.43 and 123.54 μg/mL concentration respectively, which were moderately cytotoxic as described before. This resulted may be due to the presence of phenolic and anti-tumor components of this plant [72].

Molecules that target a wide variety of complex diseases are usually designed with molecular docking in mind [73]. The function of docking is to infer the actual orientation and binding strength of a ligand within a binding pocket of the protein. It enables rationalization of the structure-activity connections of molecules derived from nature as well as contextualization of their mechanisms of action [74]. From this perspective, we applied an in-silico molecular docking approach intending to investigate the potential phytochemicals mediating antioxidant, anti-inflammatory, anti-arthritic, and cytotoxic activities of *C. rosea* as well as to explore the possible molecular mechanism of action. Consequently, five phytocompounds that were previously identified from C. *rosea* were subjected to dock against several proteins which are the major therapeutic targets for antioxidants, anti-arthritic, anti-inflammatory, and anticancer drugs. In our investigation, the overall analysis of our docking experiment exposed multiple potential compounds with high-affinity against single or multiple targets. Among them rutin was analyzed to possess a strong binding affinity against most of the target proteins implicated in the pathophysiology of oxidative stress (Fig. 5c), arthritis (Fig. 7a), inflammation (Fig. 6a), and cancer (Fig. 8c). Indeed, rutin has previously been reported to possess potent antioxidative, anti-arthritic, anti-inflammatory, antitumor, etc. effects[75–78]. Past studies indicate that beta-sitosterol and stigmasterol have a wide spectrum of biological functions, including antioxidant, immunomodulatory, anticancer, and anti-inflammatory effects [79–81]. Therefore, these compounds may be directly responsible for the observed antioxidant, anti-arthritic, anti-inflammatory, and cytotoxic activities of the C. *rosea* via interacting with the target enzyme or receptor. In addition to pharmacological profiles, ADME/T characteristics of the drug candidates are considered to be a crucial determinant of their clinical effectiveness [82]. In this context, we further explored the ADME/T profiles of the compounds through the SwissADME and admetSAR online servers. The oral bioavailability properties of the compounds were interpreted based on the physicochemical properties set out in Lipinski's rules of five. The physicochemical properties of guanidine were evaluated to satisfy Lipinski's rule of five; however, beta-sitosterol, daucosterol, stigmasterol, and rutin violated 2–4 of Lipinski's rules of five. It has been previously reported that a significant number of natural products are biologically active and have desirable pharmacokinetic properties, although they do not always fulfill the suggested "drug-likeness" parameters [83]. The admetSAR program has been employed to assess the toxicological profiles of the selected components based on the following criteria: acute oral toxicity, ames toxicity, carcinogenicity, and rat acute toxicity. Total toxicological analysis of the compounds demonstrated that the compounds do not pose a risk of acute oral toxicity, ames toxicity, carcinogenicity or rat acute toxicity. The outcome of this in-silico analysis concerning the interactions of these potential bioactive compounds from C. *rosea* with selected target enzymes and receptors indicates that these compounds could be promising therapeutic candidates for oxidative stress, arthritis, inflammation, and cancer diseases.

The optimized structural analysis of a candidate is crucial to determining stable molecular conformation in the absence of crystallographic structure. The composition and dimensionality of the 3D structures have an impact on the magnitude of the dipole moment, which provides information on the charge separation in a molecule. The dipole moment increases when the electronegativities of the attached atoms differ more. And, a low value for the dipole moment suggests that the molecule may remain as the solid state and optically inactive [84]. In our screening, five selected compounds were determined to have low dipole moments, which suggests that the molecule is slightly polar by nature. Various solvents, including chloroform, ethanol, methanol, and water, have different effects on a molecule's dipole moment depending on its environment. The molecular electrostatic potential (MESP) has been applied to analyze and forecast noncovalent interactions as well as intermolecular interactions that are vulnerable to electrophilic or nucleophilic assault [85–87]. Therefore, significant advancements in computational analysis are now being employed to provide in-depth information for investigations of chemical reactivity (e.g., hydrogen bonding interaction & biological recognition technique), zeolite, molecular clusters, and crystal behavior, as well as the prediction and correlation of a variety of macroscopic characteristics [88]. Also, Frontier molecular orbitals (FMOs) are crucial for determining the optical and electric characteristics, information on molecular reactivity, molecular structure and kinetic stability, how a molecule interacts with other species, and descriptors of chemical reactivity, such as softness and hardness [89–91]. A molecule with a narrow frontier orbital gap typically highly polarizable and chemically reactive. Low kinetic stability molecules is considered to be soft, whereas one with a high value of the frontier orbital gap is indicated to be hard and exhibit great chemical stability [92]. In our investigation, The potential values for five isolated compounds such as Rutin, Daucosterol, β-Sitosterol, Stigmasterol and Guanidine range from $-8.481e^{-2}$ a.u to $+8.481e^{-2}$ a.u, $-6.995e^{-2}$ a.u to $+6.995e^{-2}$ a.u, $-6.100e^{-2}$ a.u to $+6.100e^{-2}$ a.u, $-6.340e^{-2}$ a.u to $+6.340e^{-2}$ a.u, and $-7.382e^{-2}$ a.u to $+7.382e^{-2}$ a.u respectively; and all compound are compatible for both electrophilic and nucleophilic reactions. In addition, Rutin manifested highest reactivity among five identified isolated molecules.

5. Conclusion

The assembling pharmacological result reflects that this plant possesses the potential source of biologically active compounds, which may provide the novel healing properties upon inflammation and arthritic disorder. In our inquiry, MECR demonstrated maximum activity of anti-inflammatory and anti-oxidant with moderate toxicity. Collectively, all those outcomes of this investigation indicated the folkloric properties of this plant. In silico study is only a kind of predicting the pharmacological activity of chemical compounds, and some of the compounds showed better docking scores compared to the standard drug used in the different activity. The selected compounds did not show any carcinogenic properties. In the MESP calculations, the O-H portions of selected compounds

could provide a potential active protein binding site as well as a electrophilic & nucleophilic attacking site. Moreover, the charge transfer within the molecule, which provides the bioactive property of the compound, was investigated using the HOMO-LUMO energy values measurement; in which rutin shown the highest reactivity among other molecules. Hence, further in-depth *in-vivo* studies should be carried out to analyze the efficacy in animal model.

Research funding

None declared.

Ethical approval

Animal handling ethics were upheld in accordance with the rules of the P&D Committee of the Department of Pharmacy (P&D150/20–2019), International Islamic University Chittagong.

CRediT authorship contribution statement

Nasim Sazzad: Writing – original draft, Methodology, Investigation, Formal analysis, Conceptualization. **Fowzul Islam Fahad:** Methodology, Investigation, Data curation, Conceptualization. **Shahenur Alam Sakib:** Software, Methodology, Investigation, Data curation, Conceptualization. **Mohammed Abu Tayab:** Writing – original draft, Methodology. **Md. Abu Hanif:** Methodology, Formal analysis. **A.S.M. Ali Reza:** Supervision, Resources, Funding acquisition. **Mohammad Nazmul Islam:** Writing – original draft, Supervision, Resources, Project administration, Funding acquisition, Writing – review & editing. **Raffaele Capasso:** Writing – review & editing, Supervision.

Declaration of competing interest

The authors declare that they have no known competing financial interests or personal relationships that could have appeared to influence the work reported in this paper.

Acknowledgments

Authors are gratefully acknowledged for research facilities and other logistic supports by Department of Pharmacy, International Islamic University Chittagong (IIUC), Bangladesh; and to the Department of Theoretical and Computational Chemistry, University of Dhaka, Dhaka-1000, Bangladesh, for providing Gaussian 09 software package to carry out DFT investigations.

Abbreviations

OS	Oxidative Stress
TCA	Trichloroacetic acid
UV	Ultra-violet
MECR	Methanol extract of *Canavalia rosea*
CFCR	Chloroform fraction of *Canavalia rosea*
NFCR	N-hexane fraction of *Canavalia rosea*
HPETEs	Hydro-peroxy-eicosatetraenoic acids
NSAIDs	non-steroidal anti-inflammatory drugs
LOXs	Lipoxygenases
ADME/T	Absorption, Distribution, Metabolism, Excretion and Toxicity Analysis

Appendix A. Supplementary data

Supplementary data to this article can be found online at https://doi.org/10.1016/j.heliyon.2024.e38541.

References

[1] B. Commoner, J. Townsend, G.E. Pake, Free radicals in biological materials, Nature 174 (4432) (1954) 689–691.
[2] J.M. McCord, The evolution of free radicals and oxidative stress, Am. J. Med. 108 (8) (2000) 652–659.
[3] F.I. Fahad, et al., Investigation of the Pharmacological Properties of Lepidagathis hyalina Nees through Experimental Approaches, vol. 11, 2021, p. 180, 3.
[4] R. Rowman, The blood and bone marrow, in: Muir's Textbook of Pathology, 13th Ed., Thomas Press Ltd, India, 1966, pp. 585–644.
[5] R. Vadivu, K. Lakshmi, In vitro and in vivo anti-inflammatory activity of leaves of Symplocos cochinchinensis (Lour) Moore ssp Laurina, Bangladesh Journal of Pharmacology 3 (2) (2008) 121–124.
[6] W. Hassan, et al., Association of Oxidative Stress to the Genesis of Anxiety: Implications for Possible Therapeutic Interventions, vol. 12, 2014, pp. 120–139, 2.

[7] R. Wisastra, F.J. Dekker, Inflammation, cancer and oxidative lipoxygenase activity are intimately linked, Cancers 6 (3) (2014) 1500–1521.
[8] A.R. Brash, Lipoxygenases: occurrence, functions, catalysis, and acquisition of substrate, J. Biol. Chem. 274 (34) (1999) 23679–23682.
[9] V.J.S. Reddy, P. Rao, G.R. Lakshmi, A review on antiarthritic activity of some medicinal plants, J. Global Trends Pharmaceut. Sci. 5 (4) (2014) 2061–2073.
[10] J.-M. Kong, et al., Recent advances in traditional plant drugs and orchids, Acta Pharmacol. Sin. 24 (1) (2003) 7–21.
[11] S. Mohajer, et al., Baybean (Canavalia rosea (Sw.) DC.); organogenesis, morphological and anatomical studies, Gayana. Bot. 74 (2017) 1.
[12] K.B. Tijani, et al., Phytochemical and nutraceutical potentials of beach bean (Canavalia rosea SW.) DC grown in Anyigba, Kogi state, Nigeria, Asian Journal of Medicine and Health (2019) 1–9.
[13] S.M. Kupchan, G. Tsou, C.W. Sigel, Datiscacin, a novel cytotoxic cucurbitacin 20-acetate from Datisca glomerata, J.T.j.o.o.c. 38 (7) (1973) 1420–1421.
[14] B.C. VanWagenen, et al., Ulosantoin, a potent insecticide from the sponge Ulosa ruetzleri, J. Org. Chem. 58 (2) (1993) 335–337.
[15] A. Harborne, Phytochemical Methods a Guide to Modern Techniques of Plant Analysis, springer science & business media, 1998.
[16] M. Oyaizu, Studies on products of browning reaction antioxidative activities of products of browning reaction prepared from glucosamine, J.T.J.j.o.n. and dietetics 44 (6) (1986) 307–315.
[17] S. Vl, Analysis of total phenols and other oxidation substrates and antioxidants by means of Folin-Ciocalteu reagent, J.M.i.E. 299 (1999) 152–178.
[18] C.-C. Chang, et al., Estimation of Total Flavonoid Content in Propolis by Two Complementary Colorimetric Methods, vol. 10, 2002, 3.
[19] U. Shinde, et al., Membrane Stabilizing Activity—A Possible Mechanism of Action for the Anti-inflammatory Activity of Cedrus deodara Wood Oil, vol. 70, 1999, pp. 251–257, 3.
[20] S. Islam, et al., Evaluation of Antioxidant, Cytotoxic, Anti-inflammatory, Antiarthritic, Thrombolytic, and Anthelmintic Activity of Methanol Extract of Lepidagathis hyalina Nees Root, vol. 2022, 2022.
[21] B. Meyer, et al., Brine Shrimp: a Convenient General Bioassay for Active Plant Constituents, vol. 45, 1982, pp. 31–34, 05.
[22] D. Pattamadilok, et al., Canarosine: A New Guanidine Alkaloid from Canavalia rosea with Inhibitory Activity on Dopamine D1 Receptors, vol. 10, 2008, pp. 915–918, 10.
[23] H.M. Berman, et al., The protein data bank, Nucleic Acids Res. 28 (1) (2000) 235–242.
[24] J.-P. Declercq, et al., Crystal structure of human peroxiredoxin 5, a novel type of mammalian peroxiredoxin at 1.5 Å resolution, J. Mol. Biol. 311 (4) (2001) 751–759.
[25] C. Evrard, et al., Crystal structure of a dimeric oxidized form of human peroxiredoxin 5, J. Mol. Biol. 337 (5) (2004) 1079–1090.
[26] C. Evrard, et al., Crystal structure of the C47S mutant of human peroxiredoxin 5, J. Chem. Crystallogr. 34 (8) (2004) 553–558.
[27] P. Gouet, et al., Ferryl intermediates of catalase captured by time-resolved Weissenberg crystallography and UV-VIS spectroscopy, Nat. Struct. Biol. 3 (11) (1996) 951–956.
[28] H.-S. Shieh, et al., High resolution crystal structure of the catalytic domain of ADAMTS-5 (aggrecanase-2), J. Biol. Chem. 283 (3) (2008) 1501–1507.
[29] S.J. Taylor, et al., Fragment-based discovery of indole inhibitors of matrix metalloproteinase-13, J. Med. Chem. 54 (23) (2011) 8174–8187.
[30] M.J. Lucido, et al., Crystal structure of aspirin-acetylated human cyclooxygenase-2: insight into the formation of products with reversed stereochemistry, Biochemistry 55 (8) (2016) 1226–1238.
[31] J. Key, et al., Principles of ligand binding within a completely buried cavity in HIF2α PAS-B, J. Am. Chem. Soc. 131 (48) (2009) 17647–17654.
[32] B. Korkmaz, et al., Structure-based design and in vivo anti-arthritic activity evaluation of a potent dipeptidyl cyclopropyl nitrile inhibitor of cathepsin C, Biochem. Pharmacol. 164 (2019) 349–367.
[33] R.G. Kurumbail, et al., Structural basis for selective inhibition of cyclooxygenase-2 by anti-inflammatory agents, Nature 384 (6610) (1996) 644–648.
[34] L. Dong, et al., Fatty acid binding to the allosteric subunit of cyclooxygenase-2 relieves a tonic inhibition of the catalytic subunit, J. Biol. Chem. 291 (49) (2016) 25641–25655.
[35] S.W. Rowlinson, et al., A novel mechanism of cyclooxygenase-2 inhibition involving interactions with Ser-530 and Tyr-385, J. Biol. Chem. 278 (46) (2003) 45763–45769.
[36] G. Rimon, et al., Coxibs interfere with the action of aspirin by binding tightly to one monomer of cyclooxygenase-1, in: Proceedings of the National Academy of Sciences, vol. 107, 2010, pp. 28–33, 1.
[37] J. Stamos, M.X. Sliwkowski, C. Eigenbrot, Structure of the epidermal growth factor receptor kinase domain alone and in complex with a 4-anilinoquinazoline inhibitor, J. Biol. Chem. 277 (48) (2002) 46265–46272.
[38] X. Zhang, et al., An allosteric mechanism for activation of the kinase domain of epidermal growth factor receptor, Cell 125 (6) (2006) 1137–1149.
[39] A.D. Etoposide, Structural basis of type II topoisomerase inhibition by the, Proc. Natl. Acad. Sci. USA 102 (2005) 3703.
[40] I. Evnouchidou, et al., A common SNP in ER aminopeptidase 2 induces a specificity switch that leads to altered antigen processing, J. Immunol. 189 (5) (2012) 2383.
[41] E. Zervoudi, et al., Rationally designed inhibitor targeting antigen-trimming aminopeptidases enhances antigen presentation and cytotoxic T-cell responses, in: Proceedings of the National Academy of Sciences, vol. 110, 2013, pp. 19890–19895, 49.
[42] H.A. Hussein, et al., PockDrug-Server: a new web server for predicting pocket druggability on holo and apo proteins, Nucleic Acids Res. 43 (W1) (2015) W436–W442.
[43] R.A. Friesner, et al., Glide: a new approach for rapid, accurate docking and scoring. 1. Method and assessment of docking accuracy, J. Med. Chem. 47 (7) (2004) 1739–1749.
[44] D. Butina, M.D. Segall, K. Frankcombe, Predicting ADME properties in silico: methods and models, Drug Discov. Today 7 (11) (2002) S83–S88.
[45] E.F. Plinski, S. Plinska, Veber's Rules in Terahertz Light, 2020.
[46] F. Cheng, et al., admetSAR: a Comprehensive Source and Free Tool for Assessment of Chemical ADMET Properties, ACS Publications, 2012.
[47] M. Frisch, Gaussian 09, Gaussian, Inc., Pittsburgh, PA, Search PubMed;(b) Dalton 2.0 Program Package, 2009.
[48] R. Dennington, T.A. Keith, J.M. Millam, GaussView, Version 6.0. 16, Semichem Inc Shawnee Mission KS, 2016.
[49] A.D. Becke, Becke's three parameter hybrid method using the LYP correlation functional, J. Chem. Phys. 98 (492) (1993) 5648–5652.
[50] C. Lee, W. Yang, R.G. Parr, Development of the Colle-Salvetti correlation-energy formula into a functional of the electron density, Phys. Rev. B 37 (2) (1988) 785.
[51] B. Miehlich, et al., Results obtained with the correlation energy density functionals of Becke and Lee, Yang and Parr, Chem. Phys. Lett. 157 (3) (1989) 200–206.
[52] A.D. Becke, Basis-set-free density-functional quantum chemistry, Int. J. Quant. Chem. 36 (S23) (1989) 599–609.
[53] M. Sheikhi, D. Sheikh, Quantum chemical investigations on phenyl-7, 8-dihydro-[1, 3]-dioxolo [4, 5-g] quinolin-6 (5h)-one, Rev. Roum. Chem. 59 (9) (2014) 761–767.
[54] M.J. Balunas, A.D. Kinghorn, Drug discovery from medicinal plants, Life Sci. 78 (5) (2005) 431–441.
[55] D.E. Okwu, N.F. Uchenna, Exotic multifaceted medicinal plants of drugs and pharmaceutical industries, Afr. J. Biotechnol. 8 (25) (2009).
[56] S. Prasad, et al., Effect of Fagonia arabica (Dhamasa) on in vitro thrombolysis, BMC Compl. Alternative Med. 7 (1) (2007) 1–6.
[57] J. Wilhelm, et al., Oxidative stress in the developing rat brain due to production of reactive oxygen and nitrogen species, Oxid. Med. Cell. Longev. (2016) 2016.
[58] M.N. Islam, et al., Superoxide Dismutase: an Updated Review on its Health Benefits and Industrial Applications, vol. 62, 2022, pp. 7282–7300, 26.
[59] B. Guha, et al., Unveiling pharmacological studies provide new insights on Mangifera longipes and Quercus gomeziana, Saudi J. Biol. Sci. 28 (1) (2020) 183–190.
[60] P. Iacopini, et al., Catechin, epicatechin, quercetin, rutin and resveratrol in red grape: content, in vitro antioxidant activity and interactions, J. Food Compos. Anal. 21 (8) (2008) 589–598.
[61] A. Rakib, et al., Immunoinformatics-guided design of an epitope-based vaccine against severe acute respiratory syndrome coronavirus 2 spike glycoprotein, Comput. Biol. Med. 124 (2020) 103967.
[62] N. Banu, et al., Insightful valorization of the biological activities of Pani Heloch leaves through experimental and computer-aided mechanisms, Molecules 25 (21) (2020) 5153.

[63] M.M. Miah, et al., In vitro antioxidant, antimicrobial, membrane stabilization and thrombolytic activities of Dioscorea hispida Dennst, European Journal of Integrative Medicine 19 (2018) 121–127.
[64] A. Manikandan, et al., Efficacy of phenyl quinoline phenol derivatives as COX-2 inhibitors; an approach to emergent the small molecules as the anti-inflammatory and analgesic therapeutics, Inflammopharmacology 25 (6) (2017) 621–631.
[65] E. Umapathy, et al., An experimental evaluation of Albuca setosa aqueous extract on membrane stabilization, protein denaturation and white blood cell migration during acute inflammation, J. Med. Plants Res. 4 (9) (2010) 789–795.
[66] Y. Mizushima, Inhibition of protein denaturation by antirheumatic or antiphlogistic agents, Arch. Int. Pharmacodyn. Ther. 149 (1964) 1–7.
[67] J.R. Vane, Inhibition of prostaglandin synthesis as a mechanism of action for aspirin-like drugs, Nat. New Biol. 231 (25) (1971) 232–235.
[68] R.G. Fowles, et al., Toxicity–structure activity evaluation of limonoids from Swietenia species on Artemia salina, Pharmaceut. Biol. 50 (2) (2012) 264–267.
[69] A.L. Parra, et al., Comparative study of the assay of Artemia salina L. and the estimate of the medium lethal dose (LD50 value) in mice, to determine oral acute toxicity of plant extracts, Phytomedicine 8 (5) (2001) 395–400.
[70] A.R.M. Syahmi, et al., Acute oral toxicity and brine shrimp lethality of Elaeis guineensis Jacq.,(oil palm leaf) methanol extract, Molecules 15 (11) (2010) 8111–8121.
[71] J. Nguta, et al., Evaluation of Acute Toxicity of Crude Plant Extracts from Kenyan Biodi-Versity Using Brine Shrimp, Artemia salina L. (Artemiidae), 2012.
[72] D. Susanti, et al., Antioxidant and cytotoxic flavonoids from the flowers of Melastoma malabathricum L, Food Chem. 103 (3) (2007) 710–716.
[73] J. De Ruyck, et al., Molecular docking as a popular tool in drug design, an in silico travel, Comput. Biol. Chem. Adv. Appl.: AABC 9 (2016) 1.
[74] A.G. Atanasov, et al., Discovery and resupply of pharmacologically active plant-derived natural products: a review, Biotechnol. Adv. 33 (8) (2015) 1582–1614.
[75] J. Yang, J. Guo, J. Yuan, In vitro antioxidant properties of rutin. LWT-Food Science and Technology 41 (6) (2008) 1060–1066.
[76] A. Gul, et al., Rutin and rutin-conjugated gold nanoparticles ameliorate collagen-induced arthritis in rats through inhibition of NF-κB and iNOS activation. International immunopharmacology 59 (2018) 310–317.
[77] H. Yoo, et al., Anti-inflammatory effects of rutin on HMGB1-induced inflammatory responses in vitro and in vivo, Inflamm. Res. 63 (3) (2014) 197–206.
[78] A. Satari, et al., Rutin: a flavonoid as an effective sensitizer for anticancer therapy; insights into multifaceted mechanisms and applicability for combination therapy, Evid. base Compl. Alternative Med. 2021 (2021).
[79] S. Babu, S. Jayaraman, An update on β-sitosterol: a potential herbal nutraceutical for diabetic management, Biomed. Pharmacother. 131 (2020) 110702.
[80] S.D. Ambavade, A.V. Misar, P.D. Ambavade, *Pharmacological, nutritional, and analytical aspects of β-sitosterol: a review*. Oriental Pharmacy and Experimental Medicine 14 (3) (2014) 193–211.
[81] N. Kaur, et al., Stigmasterol: a comprehensive review, Int. J. Pharmaceut. Sci. Res. 2 (9) (2011) 2259.
[82] M.A. Tayab, et al., Antioxidant-rich woodfordia fruticosa leaf extract alleviates depressive-like behaviors and impede hyperglycemia, Plants 10 (2) (2021) 287.
[83] R.J. Quinn, et al., Developing a drug-like natural product library, J. Nat. Prod. 71 (3) (2008) 464–468.
[84] V.I. Minkin, Dipole Moments in Organic Chemistry, Springer Science & Business Media, 2012.
[85] P. Politzer, J.S. Murray, M.C. Concha, The complementary roles of molecular surface electrostatic potentials and average local ionization energies with respect to electrophilic processes, Int. J. Quant. Chem. 88 (1) (2002) 19–27.
[86] G. Naray-Szabo, G.G. Ferenczy, Molecular electrostatics, Chem. Rev. 95 (4) (1995) 829–847.
[87] J.S. Murray, P. Politzer, Statistical analysis of the molecular surface electrostatic potential: an approach to describing noncovalent interactions in condensed phases, J. Mol. Struct.: THEOCHEM 425 (1–2) (1998) 107–114.
[88] J. Gasteiger, et al., Representation of molecular electrostatic potentials by topological feature maps, J. Am. Chem. Soc. 116 (11) (1994) 4608–4620.
[89] U. Rani, et al., The spectroscopic (FTIR, FT-Raman, NMR and UV), first-order hyperpolarizability and HOMO–LUMO analysis of methylboronic acid, Spectrochim. Acta Mol. Biomol. Spectrosc. 92 (2012) 67–77.
[90] T. Karakurt, et al., Molecular structure and vibrational bands and chemical shift assignments of 4-allyl-5-(2-hydroxyphenyl)-2, 4-dihydro-3H-1, 2, 4-triazole-3-thione by DFT and ab initio HF calculations, Spectrochim. Acta Mol. Biomol. Spectrosc. 77 (1) (2010) 189–198.
[91] C.-G. Zhan, J.A. Nichols, D.A. Dixon, Ionization potential, electron affinity, electronegativity, hardness, and electron excitation energy: molecular properties from density functional theory orbital energies, J. Phys. Chem. 107 (20) (2003) 4184–4195.
[92] I. Fleming, Molecular orbitals and frontier orbitals, in: I. Fleming (Ed.), Frontier Orbitals and Organic Chemical Reactions, John Wiley and Sons, New York, 1976, pp. 5–32.